New Phytologist

Research

Elevated CO_2 induces rapid dephosphorylation of plasma membrane H^+-ATPase in guard cells

Eigo Ando[1,2], Hannes Kollist[3], Kohei Fukatsu[2], Toshinori Kinoshita[2,4] and Ichiro Terashima[1]

[1]Department of Biological Sciences, School of Science, The University of Tokyo, Hongo 7-3-1, Bunkyo, Tokyo 113-0033, Japan; [2]Division of Biological Science, Graduate School of Science, Nagoya University, Furo-cho, Chikusa, Nagoya, Aichi 464-8602, Japan; [3]Institute of Technology, University of Tartu, Tartu 50411, Estonia; [4]Institute of Transformative Bio-Molecules (WPI-ITbM), Nagoya University, Furo-cho, Chikusa, Nagoya, Aichi 464-8602, Japan

Authors for correspondence:
Eigo Ando
Email: e.ando.ac@gmail.com

Toshinori Kinoshita
Email: kinoshita@bio.nagoya-u.ac.jp

Received: *29 March 2022*
Accepted: *26 August 2022*

New Phytologist (2022) **236:** 2061–2074
doi: 10.1111/nph.18472

Key words: *Arabidopsis thaliana*, CO_2 signalling, dephosphorylation, guard cell, light–dark transition, photosynthesis, plasma membrane H^+-ATPase, stomatal closure.

Summary

- Light induces stomatal opening, which is driven by plasma membrane (PM) H^+-ATPase in guard cells. The activation of guard-cell PM H^+-ATPase is mediated by phosphorylation of the penultimate C-terminal residue, threonine. The phosphorylation is induced by photosynthesis as well as blue light photoreceptor phototropin. Here, we investigated the effects of cessation of photosynthesis on the phosphorylation level of guard-cell PM H^+-ATPase in *Arabidopsis thaliana*.
- Immunodetection of guard-cell PM H^+-ATPase, time-resolved leaf gas-exchange analyses and stomatal aperture measurements were carried out.
- We found that light–dark transition of leaves induced dephosphorylation of the penultimate residue at 1 min post-transition. Gas-exchange analyses confirmed that the dephosphorylation is accompanied by an increase in the intercellular CO_2 concentration, caused by the cessation of photosynthetic CO_2 fixation. We discovered that CO_2 induces guard-cell PM H^+-ATPase dephosphorylation as well as stomatal closure. Interestingly, reverse-genetic analyses using guard-cell CO_2 signal transduction mutants suggested that the dephosphorylation is mediated by a mechanism distinct from the established CO_2 signalling pathway. Moreover, type 2C protein phosphatases D6 and D9 were required for the dephosphorylation and promoted stomatal closure upon the light–dark transition.
- Our results indicate that CO_2-mediated dephosphorylation of guard-cell PM H^+-ATPase underlies stomatal closure.

Introduction

Stomata, which are microscopic pores comprising pairs of guard cells in the plant epidermis, control leaf gas-exchange in response to various environmental and endogenous stimuli. Light stimulates stomatal opening and promotes CO_2 uptake for photosynthesis, whereas darkness, high CO_2 concentrations, low air humidity, the phytohormone abscisic acid (ABA) and drought stress induce stomatal closure to prevent excess water loss via transpiration (Roelfsema *et al.*, 2012; Inoue & Kinoshita, 2017; Jezek & Blatt, 2017; Lawson & Matthews, 2020).

Red and blue light induce stomatal opening via photosynthesis- and phototropin-dependent mechanisms. Stomatal opening mediated by blue light-activated phototropins is induced by the low fluence rate of blue light under high fluence rate of red light that saturates photosynthesis (Shimazaki *et al.*, 2007; Inoue & Kinoshita, 2017). In guard cells, phototropins mediate phosphorylation of penultimate C-terminal residue of plasma membrane (PM) H^+-ATPase, threonine (Thr), which recruits regulatory protein 14-3-3 to activate this enzyme (Kinoshita & Shimazaki, 1999, 2002; Kinoshita *et al.*, 2001). The activated PM H^+-ATPase generates a H^+ concentration gradient across the PM, which hyperpolarises the membrane potential, prompting voltage-gated K^+ channels and the H^+-coupled transporters to accumulate K^+ and other anions in guard cells. The accumulation of solutes promotes osmotic water influx into the cells and therefore stomatal opening (Roelfsema *et al.*, 2012; Inoue & Kinoshita, 2017; Jezek & Blatt, 2017). Among the 11 isoforms of PM H^+-ATPase in *Arabidopsis thaliana* (Arabidopsis; AHA1–AHA11), AHA1, which is the most abundant in guard cells, is responsible for blue light-induced stomatal opening (Yamauchi *et al.*, 2016). Recent studies revealed that clade D type 2C protein phosphatases (PP2C.Ds) regulate the phosphorylation of the penultimate residue of PM H^+-ATPase in guard cells (Wong *et al.*, 2021; Akiyama *et al.*, 2022). Phototropins also inhibit the release of anions through PM anion channels, which also contributes to PM hyperpolarisation (Marten *et al.*, 2007; Hiyama *et al.*, 2017). Triacylglycerols stored in lipid droplets in guard cells are broken down in a phototropin-dependent manner to provide ATP for PM H^+-ATPase (McLachlan *et al.*, 2016). Sugars and their metabolites may function as osmolytes and/or substrates for glycolysis and mitochondrial respiration during light-induced

stomatal opening (Daloso *et al.*, 2016; Granot & Kelly, 2019). Blue light-induced activation of PM H^+-ATPase mediates starch degradation, producing glucose in guard cells (Horrer *et al.*, 2016; Santelia & Lunn, 2017; Flütsch *et al.*, 2020).

Photosynthesis in mesophyll or guard-cell chloroplasts, or both, are involved in red light-induced stomatal opening (Mott *et al.*, 2008; Fujita *et al.*, 2013, 2019; Suetsugu *et al.*, 2014). Decreases in the intercellular CO_2 concentration (C_i) following mesophyll photosynthesis alters the activity of PM ion channels, which facilitates ion accumulation in guard cells (Brearley *et al.*, 1997; Roelfsema *et al.*, 2002; Hosotani *et al.*, 2021). Stomata also open via C_i-independent mechanisms (Messinger *et al.*, 2006; Lawson *et al.*, 2008; Matrosova *et al.*, 2015). Furthermore, photosynthesis replenishes the ATP supply to PM H^+-ATPase (Tominaga *et al.*, 2001; Suetsugu *et al.*, 2014; Wang *et al.*, 2014) and is a source of sucrose in guard cells (Flütsch *et al.*, 2020). Red light induces photosynthesis-dependent phosphorylation of the penultimate residue of PM H^+-ATPase in Arabidopsis guard cells (Ando & Kinoshita, 2018). Moreover, red-light-induced stomatal opening is suppressed in mutant plants lacking *AHA1* (Yamauchi *et al.*, 2016; Ando & Kinoshita, 2018; Flütsch *et al.*, 2020). Therefore, PM H^+-ATPase activity is likely to be required for both blue and red-light-induced stomatal opening.

The mechanisms driving dark-induced stomatal closure are poorly understood. Various factors affecting stomatal aperture in the dark have been identified in guard cells, including transcriptional regulation (Liang *et al.*, 2005), the mitochondria-mediated cytosolic ATP concentration (Goh *et al.*, 2011), the cytoskeleton (Eisinger *et al.*, 2012; Isner *et al.*, 2017), photomorphogenesis (Mao *et al.*, 2005; Khanna *et al.*, 2014), and cytosolic pH-dependent control of reactive oxygen species levels (Desikan *et al.*, 2004; She *et al.*, 2010; Ma *et al.*, 2012). However, the early molecular processes involved in dark-induced stomatal closure remain elusive.

When the plants are transferred to dark conditions, photosynthesis ceases and CO_2 is emitted by respiration, and transiently by photorespiration (post-illumination CO_2 burst) in the leaves; therefore, dark-induced stomatal closure may be partly mediated by CO_2 (Engineer *et al.*, 2016; Zhang *et al.*, 2018; Chikov & Akhtyamova, 2019). Previous studies on CO_2-induced stomatal closure focused on the activation of PM anion channels in guard cells. In Arabidopsis, beta carbonic anhydrases, CARBONIC ANHYDRASE1 (CA1) and CA4 convert CO_2 into bicarbonate (Hu *et al.*, 2010; Xue *et al.*, 2011), which inactivates the protein kinase HIGH LEAF TEMPERATURE1 (HT1; Hashimoto *et al.*, 2006), a negative regulator of slow-type anion channels in PM in guard cells (Tian *et al.*, 2015; Hõrak *et al.*, 2016; Tõldsepp *et al.*, 2018). CONVERGENCE OF BLUE LIGHT AND CO_2 1 (CBC1) and CBC2 may be activated by HT1 to suppress the activities of PM anion channels (Hiyama *et al.*, 2017). Activation of PM anion channels promotes the release of anions from guard cells, which causes PM depolarisation and drives K^+ release through outward-rectifying voltage-gated K^+ channels in guard cells, leading to osmotic water efflux from the cells and stomatal closure (Roelfsema *et al.*, 2012; Jezek & Blatt, 2017). Indeed, plants lacking anion channels exhibited delayed stomatal closure in response to dark conditions (Negi *et al.*, 2008; Vahisalu *et al.*, 2008; Jalakas *et al.*, 2021). Moreover, CO_2 may inhibit PM H^+ extrusion pumps in guard cells (Edwards & Bowling, 1985), implying that dark-induced stomatal closure involves the CO_2-mediated inhibition of PM H^+-ATPase in guard cells; however, molecular evidence for this hypothesis is lacking.

In this study, we found that light–dark transition induces the dephosphorylation of guard-cell PM H^+-ATPase within 1 min in Arabidopsis leaves, accompanied by an increase in C_i caused by the cessation of photosynthesis. Inspired by this finding and the hypothesis that CO_2 may inhibit PM H^+-ATPase in guard cells (Edwards & Bowling, 1985), we conducted physiological and reverse-genetic analyses using CO_2 signal transduction mutants to characterise the dephosphorylation of PM H^+-ATPase. We also investigated the potential involvement of PP2C.Ds in rapid dephosphorylation and stomatal closure upon the light–dark transition. Our results indicate that elevated CO_2 induces the dephosphorylation of guard-cell PM H^+-ATPase, which facilitates stomatal closure.

Materials and Methods

Plant materials and growth conditions

Arabidopsis Columbia-0 (Col-0) was used as the wild-type in physiological experiments. Col-0 was also used as the control for *blue light-dependent h$^+$-atpase phosphorylation-1* (*bhp-1*; Hayashi *et al.*, 2017), *ca1 ca4* (Hu *et al.*, 2010), *cbc1 cbc2* (Hiyama *et al.*, 2017), *ht1-8D* (Hõrak *et al.*, 2016), *ht1-9* (Hiyama *et al.*, 2017), *open stomata1-3* (*ost1-3*; Yoshida *et al.*, 2002) and *pp2c.ds* (Akiyama *et al.*, 2022). Landsberg *erecta* (L*er*) was used as the control for *ost2-1* (Merlot *et al.*, 2007). Plants were grown in soil in a growth room or chamber. The light regime, growth temperature and relative humidity were set to a 16-h photoperiod with a white fluorescence lamp (*c.* 50 μmol m^{-2} s^{-1}), 20–24°C and 40–60%, respectively. Plants grown for 4–6 wk were kept in the dark overnight and fully expanded mature leaves were used for the experiments.

Light sources

Light-emitting photodiodes (ISL-150X150-H4RHB; CCS) with a power supply (ISC-201-2; CCS) were used as the light source, except for in the experiment for Fig. 2 (please refer to later paragraphs), in which a halogen projector lamp (6423; Philips, Amsterdam, the Netherlands) with a red filter (2–61; Corning Inc., Corning, NY, USA) and power supply (MHAB-150 W; Moritex, Saitama, Japan) was used. Photon flux densities were measured with a light analyser (LA-105; NK System, Osaka, Japan).

Treatments for immunohistochemical analyses and stomatal aperture measurements

Leaves collected from dark-treated plants were put on Mill-Q water (Millipore, Burlington, MA, USA) and treated as indicated. Isolated epidermal fragments were prepared from the dark-

treated leaves by blending the leaves for < 5 s twice in Milli-Q water with a blender (7011HS; Waring Commercial) equipped with a container (MC-1; Waring Commercial, Stamford, CT, USA) at high speed. The epidermal fragments were collected on 59-μm nylon mesh and incubated in a buffer comprising 5 mM 2-ethanesulfonic acid (MES)-BTP (pH 6.5), 50 mM KCl and 0.1 mM $CaCl_2$. For bicarbonate treatment experiments, the concentration of MES and the buffer pH were adjusted to 20 mM and pH 5.5, respectively. $NaHCO_3$ or Na_2HPO_4 dissolved in Mill-Q water was added to the buffer at concentrations of 2.5 and 1.25 mM, respectively. The final volume of water added to the buffer was 0.27% (v/v).

Immunohistochemical analyses of guard-cell PM H^+-ATPase in leaves

The immunohistochemical analyses using leaves were performed according to the previous method with slight modifications (Ando & Kinoshita, 2018). In brief, leaves were chemically fixed with 4% (w/v) formaldehyde (prepared from paraformaldehyde, Wako, Osaka, Japan) and 0.3% (w/w) glutaraldehyde (Nacalai Tesque, Kyoto, Japan) in microtubule-stabilising buffer (MTSB; 50 mM PIPES-NaOH (pH 7.0), 5 mM $MgSO_4$, 5 mM EGTA) for 1 h at room temperature in the dark. Before incubation with the fixative, the leaves were infiltrated with the same solution within 20 s after the light treatments. After washing with phosphate-buffered saline (PBS; 137 mM NaCl, 8.1 mM Na_2HPO_4, 2.68 mM KCl and 1.47 mM KH_2PO_4), the leaves were incubated with pure methanol to remove Chl. The leaves were further incubated with pure xylene for 2 min at 37°C, ethanol for 5 min at room temperature and 50% ethanol (v/v; in PBS) for 5 min at room temperature, then washed with Milli-Q water for 5 min twice and mounted on MAS-coated microscope slides (Matsunami). Five times freeze–thawed cycles using liquid nitrogen were applied to the leaves. The specimens were digested with 1% (w/v) Cellulase R-10 and 0.5% (w/v) Macerozyme R-10 (Yakult) in PBS (pH 6.0; adjusted by HCl) for 1 h at 37°C, then leaf tissue except abaxial epidermis attached to the slide was removed. The epidermis left on the slide was permeabilised with 3% (v/v) Igepal CA-630 (MP Biochemicals) and 10% (v/v) dimethyl sulfoxide in PBS for 30 min at room temperature. After 1-h blocking with 3% (w/v) bovine serum albumin fraction V in PBS (Gibco; Thermo Fisher Scientific, Waltham, MA, USA), the primary antisera against the conserved catalytic domain of PM H^+-ATPase (anti-H^+-ATPase) or its C-terminal phosphorylated residue, threonine (anti-pThr; Hayashi *et al.*, 2010), was applied at a dilution of 1 : 2000 in the blocking solution for overnight at 4°C. Alexa Fluor 488-conjugated secondary antibody (A11034; Invitrogen) was applied at a dilution of 1 : 500 in the blocking solution for 3 h at 37°C.

Immunohistochemical analyses of guard-cell PM H^+-ATPase in epidermal fragments

The immunohistochemical analyses using epidermal fragments were performed as described previously (Hayashi *et al.*, 2011; Ando & Kinoshita, 2018). In brief, epidermal fragments were fixed with 4% (w/v) formaldehyde with 0.1% (w/w) glutaraldehyde for 2 h at 4°C. After washing, epidermal fragments were transferred to pure methanol to remove Chl, then washed with Milli-Q water and mounted on a cover glass coated with 0.1% (w/v) poly-L-lysine (Sigma-Aldrich). The specimens were digested with 3% (w/v) Driselase (Sigma-Aldrich) and 0.5% (w/v) Macerozyme R-10 in PBS for 45 min at 37°C, then permeabilised with 3% (w/w) Triton X-100 in PBS for 30 min at room temperature. Blocking and antisera application were conducted as described above.

Fluorescence microscopy

After secondary antibody application, specimens were washed and covered with 50% (v/v) glycerol. The phosphorylation levels and amounts of guard-cell PM H^+-ATPase was estimated based on Alexa Fluor 488 fluorescence intensity using ImageJ software (National Institutes of Health; Schneider *et al.*, 2012; Ando & Kinoshita, 2018). In brief, the difference between the mean grey value of guard cells and that of the neighbouring area excluding guard cells was calculated for each pair of guard cells. The difference between the geometric mean obtained for each antiserum and normal serum was calculated as net fluorescence intensity and expressed relative to corresponding control. Data are represented by the mean ± SD of at least three independent measurements.

Immunoblot analyses of PM H^+-ATPase in guard-cell protoplasts (GCPs)

GCPs were enzymatically isolated as described previously (Ueno *et al.*, 2005) with slight modifications in which 0.05% (w/v) Macerozyme R-10 and 0.0075% (w/v) pectolyase Y-23 (Kyowa Chemical Products; Kyowa Kasei Co. Ltd, Osaka, Japan) was used for first- and second-step digestion, respectively. Isolated GCPs were kept in the dark on ice until use (at least for 1 h). GCPs in a suspension buffer comprising 20 mM MES-KOH (pH 5.5), 10 mM KCl, 0.4 M mannitol and 1 mM $CaCl_2$, was stirred at 300 round min^{-1} in a glass vessel enclosed in a water jacket filled with circulating water (24°C) during the treatments. $NaHCO_3$ dissolved in the suspension buffer was applied to GCPs at a concentration of 10 mM. The final volume of the buffer added to the suspension was 1.09% (v/v). The GCPs' proteins were subjected to immunoblot analyses using primary antisera anti-H^+-ATPase and anti-pThr. 14-3-3 proteins were detected as a loading control using anti-14-3-3 antiserum (Kinoshita & Shimazaki, 1999). The protein amounts were estimated using ImageJ software based on chemiluminescence from a reaction of horseradish peroxidase-conjugated secondary antibody (1706515; Bio-Rad) with the substrate (Thermo Fisher Scientific). Data are represented by the mean ± SD of three independent measurements.

Measurement of stomatal aperture

After the treatments, epidermal fragments were collected using a nylon mesh. Leaves were collected and the epidermal

fragments were obtained as described above. Collected epidermal fragments were immediately microphotographed using a microscope (BX50; Olympus, Tokyo, Japan) equipped with a charge-coupled device (CCD) camera system (DP71; Olympus). Stomatal apertures on the abaxial side fragments were measured using ImageJ software. Representative values of independent measurements were calculated as means of at least 30 stomatal apertures. Data are provided as the means of representative values obtained in at least three independent measurements with SDs.

Gas-exchange measurements

Gas-exchange measurements were performed using the LI-6400 system (Li-Cor, Lincoln, NE, USA). Air flow rate and leaf temperature were kept at 500 μmol s^{-1} and 23°C, respectively. Relative humidity in the leaf chamber was maintained at 40–60%. C_a was set to 400 μmol mol^{-1} unless otherwise stated. After the measurements, the leaves were photographed and leaf areas were measured using ImageJ software. The recorded values were normalised to the true leaf area. Data are the mean ± SE of at least four separate leaves from individual plants.

To perform the combined gas-exchange and immunohistochemical analyses, leaves were detached from the plants and immediately infiltrated with fixative. Leaf area was measured after fixation to correct the gas-exchange measurements, as described above. The phosphorylation level and amount of guard-cell PM H^+-ATPase are represented by the mean ± SE of four independent plants.

Estimation of stomatal density

According to a previously described method (Kang *et al.*, 2009), leaves used for the gas-exchange analyses were fixed with 95% (v/v) ethanol, rehydrated in 75% (v/v), 50% (v/v) and 25% (v/v) ethanol series, washed with Milli-Q water and immersed in clearing solution (glycerol : chloral hydrate : water, 1 : 8 : 1, v/w/v). The average stomatal density of six areas of each leaf was calculated microscopically, as an estimate for the whole leaf. Data are the mean ± SE.

Statistical analyses

Means expressed as relative values were analysed by one-sample *t* tests to compare with the corresponding controls, which were set to 1. The statistical significance of the difference between two independent means was assessed using Student's *t*-test. For means expressed as absolute values, Dunnett's test was applied for comparison with a single control. The statistical significance of differences among means was assessed by Tukey's test. *P*-values were calculated in R software using the package multcomp (Hothorn *et al.*, 2008; R Core Team, 2021). The statistical significance of correlations was analysed using the R function *cor.test*. A *P*-value < 0.05 was considered statistically significant.

Results

Rapid dephosphorylation of guard-cell PM H^+-ATPase in response to the light–dark transition in leaves

Our previous immunohistochemical study using Arabidopsis leaves revealed that red light induces photosynthesis-dependent phosphorylation of the penultimate C-terminal residue of PM H^+-ATPase, Thr, in guard cells during red-light-induced stomatal opening (Ando & Kinoshita, 2018). This finding implied that the cessation of photosynthesis may affect the phosphorylation level of guard-cell PM H^+-ATPase. To test this hypothesis, we conducted immunohistochemical analyses of Arabidopsis wild-type Col-0 leaves undergoing the light–dark transition using antisera against the phosphorylated Thr of PM H^+-ATPase (Hayashi *et al.*, 2010). As the phosphorylation of PM H^+-ATPase in guard cells is mediated by both red and blue light (Inoue & Kinoshita, 2017), we first illuminated leaves with red light only (600 μmol m^{-2} s^{-1}) and then subjected them to dark treatment for 1, 5, 15 and 30 min. We observed a rapid decrease in the phosphorylation of PM H^+-ATPase in guard cells, even with only a 1-min dark treatment (Fig. 1a,b). The phosphorylation level remained low until 30 min after dark treatment (Fig. 1b). To investigate whether the decrease in phosphorylation level was caused by the change in the amount of PM H^+-ATPase itself, we conducted immunohistochemical analyses using antibodies that recognise the conserved catalytic domain of PM H^+-ATPase (Hayashi *et al.*, 2010); there was no significant difference in the amount of PM H^+-ATPase before and after dark treatment (Fig. 1c). These results indicated that dephosphorylation of PM H^+-ATPase occurred in guard cells within 1 min of dark treatment.

Next, we examined whether dark-induced rapid dephosphorylation of PM H^+-ATPase also occurred after blue light illumination. We illuminated the leaves with weak blue light (5 μmol m^{-2} s^{-1}) superimposed on the red light (600 μmol m^{-2} s^{-1}) and then turned off either the blue light only or both lights and maintained those conditions for 1 min. We found that the phosphorylation level of PM H^+-ATPase was maintained for 1 min under red light following blue light treatment (Fig. 1d,e). By contrast, when both light sources were turned off, phosphorylation decreased within 1 min, with no change in the amount of PM H^+-ATPase (Fig. 1d–f); this indicates that the rapid dark-induced dephosphorylation of PM H^+-ATPase also occurs following blue light illumination. Moreover, this rapid dephosphorylation was not observed in isolated epidermal fragments, and the dephosphorylation kinetics were comparable between red light and dark conditions (Fig. S1a). Taken together, these results indicated that guard-cell PM H^+-ATPase is rapidly dephosphorylated during the light–dark transition in the leaves of Arabidopsis. To simplify the downstream experiments, only red light was applied in those involving the light–dark transition of leaves.

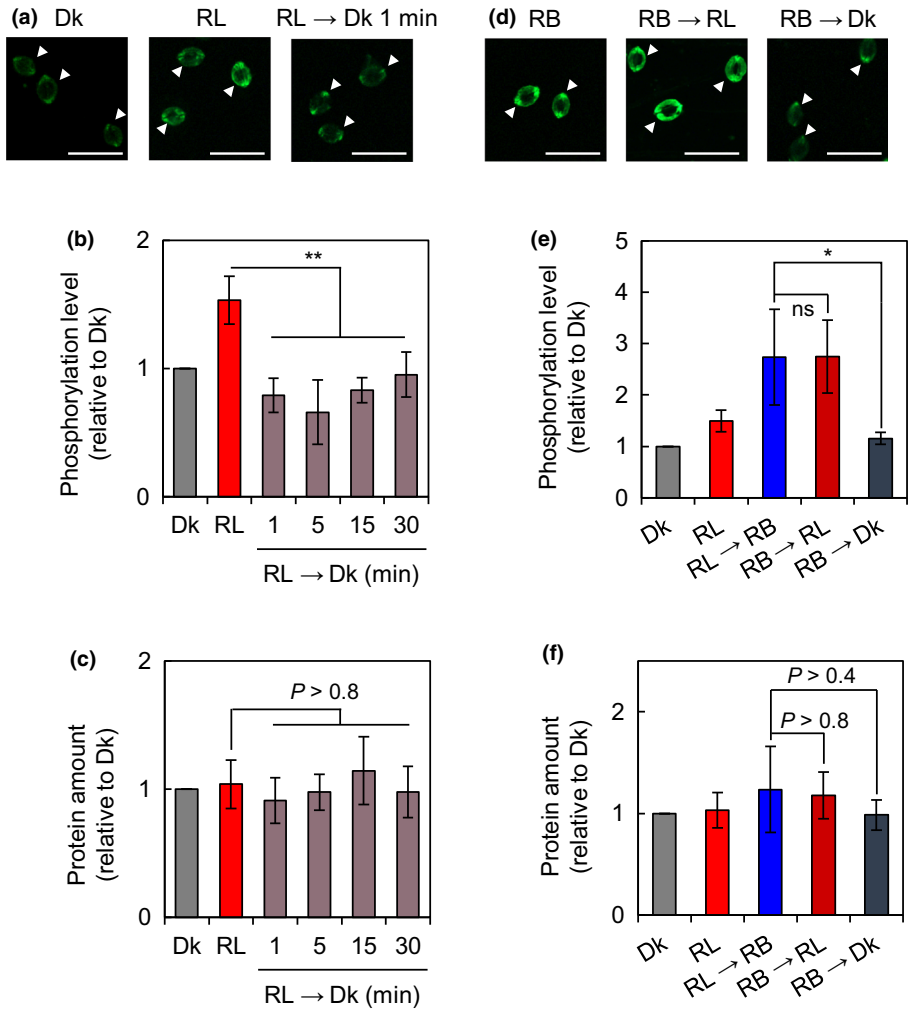

Fig. 1 Rapid dephosphorylation of guard-cell plasma membrane (PM) H^+-ATPase in *Arabidopsis thaliana* wild-type Col-0 leaves upon light–dark transition. The phosphorylation level (a–c) and amount (d–f) of PM H^+-ATPase in guard cells were analysed by applying immunohistochemical techniques to leaves. Mature leaves harvested from dark-treated plants were kept in the dark (Dk), illuminated with red light (RL; at 600 μmol m^{-2} s^{-1}) for 30 min, kept in the dark again for the indicated time (RL→Dk), illuminated with blue light (5 μmol m^{-2} s^{-1}) superimposed on red light for 2.5 min after RL (RL→RB), illuminated with red light, or kept in the dark for 1 min after RB (RB→RL, RB→Dk). (a, d) Representative fluorescence images of the phosphorylation level of PM H^+-ATPase in guard cells. Arrowheads indicate guard cells. Bar, 50 μm. (b, e) Estimation of the phosphorylation level of PM H^+-ATPase in guard cells. Asterisks indicate that the means of RL→Dk and RB→Dk are significantly lower than those of RL (b) and RL→RB (e), respectively. *, $P < 0.01$; **, $P < 0.005$; ns, not significant, $P > 0.6$ (one-tailed Dunnett's test). (c, f) Estimation of the amount of PM H^+-ATPase in guard cells. The means denoted in brackets are not statistically significantly different to that of RL (c) or RL→RB (f), as indicated by the *P*-values (two-tailed Dunnett's test). Data represent the mean ± SD relative phosphorylation level and amount of PM H^+-ATPase compared with Dk, based on three (b, c) or four (e, f) independent measurements.

Dark-induced stomatal closure follows cessation of photosynthesis and dephosphorylation of guard-cell PM H^+-ATPase and requires deactivation of PM H^+-ATPase in leaves

To examine the interrelationships among the photosynthetic rate, C_i and stomatal movement during the light–dark transition, we performed time-resolved gas-exchange analyses. As in previous studies (Engineer *et al.*, 2016; Chikov & Akhtyamova, 2019), the photosynthetic rate decreased immediately and reached its minimum value within 1 min after the light–dark transition (Fig. 2). Similarly, the C_i increased to a level slightly above the ambient CO_2 concentration (C_a) within 1 min of the light–dark transition. Stomatal conductance was maintained at 1 min after the light–dark transition and began to decrease *c.* 3 min after transfer to dark conditions. Taken together, these results suggest that the dephosphorylation of PM H^+-ATPase in guard cells is accompanied by the cessation of photosynthesis and an increase in C_i, followed by stomatal closure in the leaf after the light–dark transition.

The phosphorylation of the penultimate residue of PM H^+-ATPase, Thr, is important for the activation of this enzyme through the interaction with 14-3-3 protein in guard cells, which creates the driving force for stomatal opening (Kinoshita & Shimazaki, 1999, 2002). To genetically validate the requirement of the deactivation of PM H^+-ATPase in dark-induced stomatal closure, we compared *ost2-1*, in which AHA1 is mutated and constitutively activated (Merlot *et al.*, 2007) and corresponding control L*er* on the stomatal closure. The light–dark transition of L*er* leaves initiated decrease in the stomatal aperture within 10 min post-transition, whereas dark-induced stomatal closure was abolished in *ost2-1* leaves (Fig. S2). Therefore, deactivation of PM H^+-ATPase is most likely to be required for stomatal closure in response to the light–dark transition.

Elevated CO_2 treatment induces the dephosphorylation of PM H^+-ATPase in guard cells

The lack of rapid dark-induced dephosphorylation of guard-cell PM H^+-ATPase in isolated epidermal fragments (Fig. S1a) suggested that the rapid dephosphorylation seen in the leaf was caused by the cessation of mesophyll photosynthesis upon the light–dark transition. When mesophyll photosynthesis ceases under dark conditions, the C_i increases (Fig. 2; Engineer *et al.*,

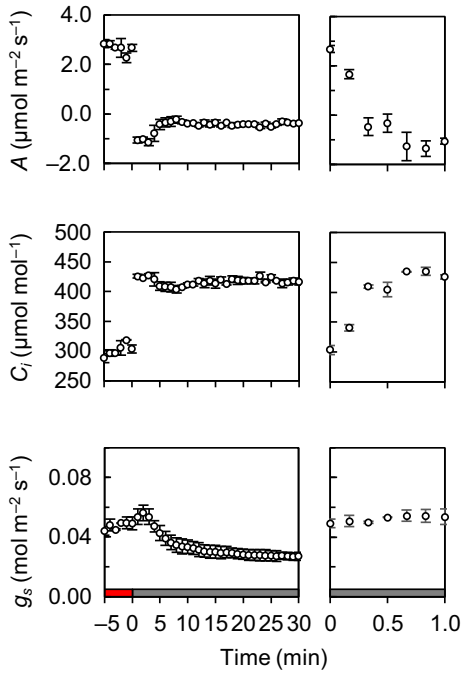

Fig. 2 Darkness triggered a decrease in the photosynthetic rate (*A*) and an increase in intercellular CO_2 concentration (C_i), followed by a decrease in stomatal conductance (g_s). *Arabidopsis thaliana* wild-type Col-0 leaves were preilluminated with red light (600 μmol m^{-2} s^{-1}) for 60 min and kept in the dark for 30 min. Grey and red bars represent darkness and red-light illumination, respectively. Right panels show measurements taken 1 min after the termination of red light. Data are the mean ± SE of three leaves taken from different plants.

2016; Chikov & Akhtyamova, 2019), while CO_2 inhibits PM H^+-ATPase in guard cells (Edwards & Bowling, 1985). This suggests that elevated C_i may induce the dephosphorylation of PM H^+-ATPase in guard cells. To test this hypothesis, we combined immunohistochemical analyses with gas-exchange measurements; leaves were treated with elevated CO_2 concentrations (eCO_2) in a leaf chamber (Figs 3a, S3) and immunohistochemical analyses were performed immediately. eCO_2 treatment was applied for 1 or 2 min, because the C_i stabilised within 2 min (Fig. S3). Without eCO_2 treatment, C_a was maintained at 400 μmol mol^{-1}, and red-light-induced phosphorylation and dark-induced dephosphorylation of PM H^+-ATPase in guard cells were both observed, along with the accompanying changes in the photosynthetic rate and C_i (Figs 3b, S3). Under the eCO_2 treatment conditions, in which C_a was raised from 400 to 800 μmol mol^{-1} under the red light, the phosphorylation level of PM H^+-ATPase decreased within 2 min; therefore, the phosphorylation level and C_i were negatively correlated under the red light (Figs 3b, S3). The amount of guard-cell PM H^+-ATPase did not differ between treatments (Fig. 3c). These results indicated that increased C_i induced the dephosphorylation of guard-cell PM H^+-ATPase in the leaves, even in the presence of red light.

In the isolated epidermal fragments, the dephosphorylation of guard-cell PM H^+-ATPase and stomatal closure occurred much more slowly (Fig. S1a,b). To further investigate whether CO_2 mediates the dephosphorylation of PM H^+-ATPase in guard cells, we examined the effects of exogenous CO_2 on stomatal response speeds in the epidermal fragments. We used sodium bicarbonate ($NaHCO_3$) as an exogenous source of CO_2 (Kolla *et al.*, 2007) and investigated its effects on stomatal responses. Epidermal fragments were suspended in buffer containing 20 mM MES (pH 5.5) and preilluminated with blue light superimposed onto red light to induce the phosphorylation of guard-cell PM H^+-ATPase (Fig. 3d, red light (RL) → red-blue (RB)), and then transferred to dark conditions with or without $NaHCO_3$ supplementation and incubated for 1 min. In the control conditions, in which the samples were treated with water or 1.25 mM disodium phosphate (Na_2HPO_4) instead of 2.5 mM $NaHCO_3$, guard-cell PM H^+-ATPase was not dephosphorylated 1 min after the light–dark transition; however, dephosphorylation was accelerated in samples treated with $NaHCO_3$ (Fig. 3d). In addition, $NaHCO_3$ induced the dephosphorylation even under blue light-illuminated conditions, albeit with slight delay (Fig. S4). Immunoblot analyses using GCPs confirmed that $NaHCO_3$ decreases the phosphorylation level relative to the protein amount without unequivocal protein degradation, which suggests that dephosphorylation rather than degradation of PM H^+-ATPase occurs in response to CO_2 (Fig. S5). These results indicated that the rapid dephosphorylation of guard-cell PM H^+-ATPase in leaves could be mimicked using $NaHCO_3$. Consistent with the phosphorylation levels of PM H^+-ATPase, the exogenous $NaHCO_3$ also enhanced dark-induced stomatal closure; the stomatal apertures decreased within 10 min of the light–dark transition (Fig. 3e). Taken together, these results demonstrated that CO_2 promotes the dephosphorylation of PM H^+-ATPase in guard cells, as well as stomatal closure, in the dark.

Carbonic anhydrases *CA1* and *CA4* are involved in dark-induced dephosphorylation of PM H^+-ATPase in guard cells

Our results suggest that the molecular mechanism driving rapid dark-induced dephosphorylation of PM H^+-ATPase may share signalling components with CO_2-induced stomatal closure (Zhang *et al.*, 2018; Dubeaux *et al.*, 2021). Therefore, we applied a reverse-genetic approach. We first investigated whether the beta carbonic anhydrases *CA1* and *CA4*, which are early signalling components in CO_2-induced stomatal closure (Hu *et al.*, 2010), are required for dephosphorylation. We found that the phosphorylation level of guard-cell PM H^+-ATPase was two-fold higher in *ca1 ca4* mutants compared with the wild-type, in dark-treated leaves (Fig. 4a, dark (Dk)). Red-light illumination induced further phosphorylation of PM H^+-ATPase in the leaves of *ca1 ca4*; the PM H^+-ATPase phosphorylation level was *c.* 64% higher in the mutant compared with the wild-type under RL (Fig. 4a, RL). Red light–dark transition did not induce rapid dephosphorylation of PM H^+-ATPase in *ca1 ca4* leaves (Fig. 4a, RL→Dk). The amount of PM H^+-ATPase in guard cells was comparable between *ca1 ca4* and the wild-type (Fig. 4b). Furthermore, eCO_2-induced dephosphorylation was impaired in *ca1 ca4* leaves (Fig. S6). These results indicated that *CA1* and *CA4* are required for the rapid dephosphorylation of guard-cell PM H^+-ATPase upon the light–dark transition or C_i elevation.

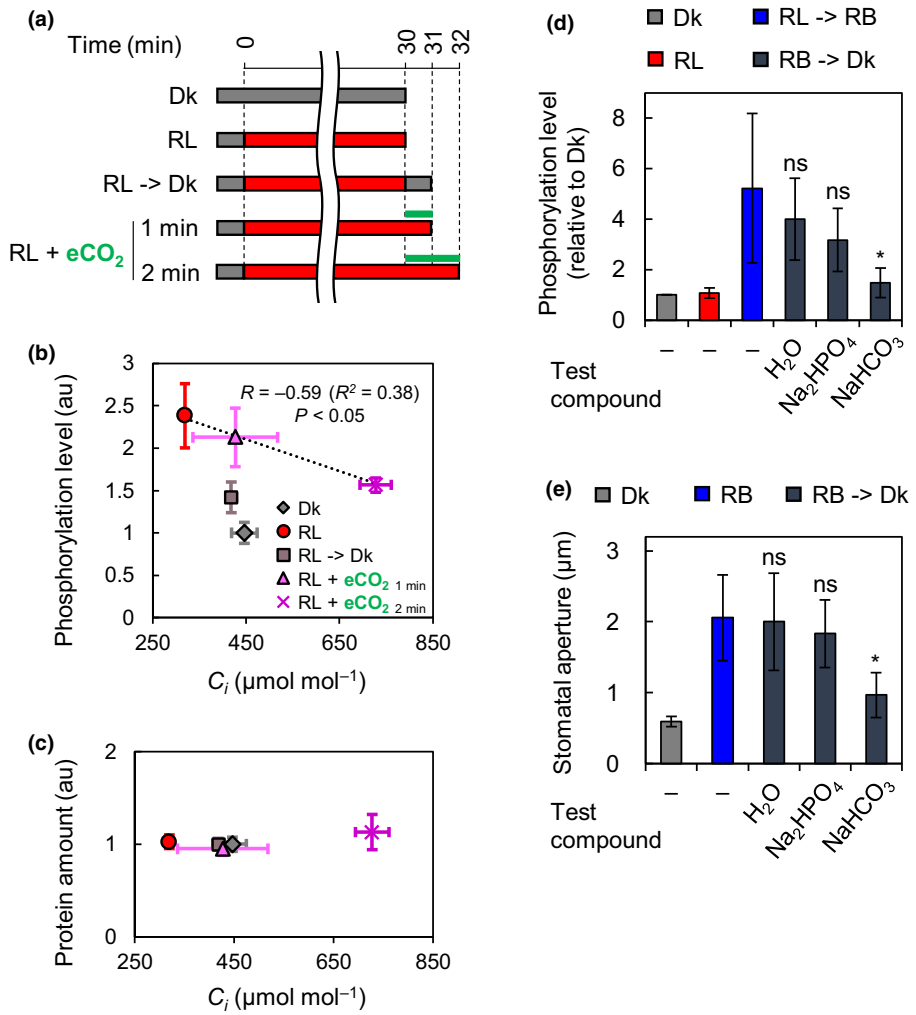

Fig. 3 CO_2 induces dephosphorylation of guard-cell plasma membrane (PM) H^+-ATPase in *Arabidopsis thaliana* wild-type Col-0. (a–c) Elevated CO_2 (eCO_2) treatment to the leaves under red light. (a) Schematic diagram of the treatment conditions. Grey and red bars represent dark and red-light illumination (600 μmol m^{-2} s^{-1}) conditions, respectively. Green lines represent exposure to eCO_2 (up to 800 μmol^{-1}). Leaves from dark-treated plants were treated as indicated in the leaf chamber of the gas-exchange measurement system. (b, c) Relationships between the phosphorylation level (b) and amount (c) of guard-cell PM H^+-ATPase estimated by immunohistochemical analyses and the intercellular CO_2 concentration (C_i) at the time of leaf harvesting. There was a significant negative correlation between the phosphorylation level and C_i under red light (dotted line). Data represent the mean ± SE of four leaves taken from different plants. The gas-exchange measurements recorded in this experiment are shown in Fig. S2. (d, e) Exogenous bicarbonate treatment to the isolated epidermal fragments upon the light–dark transition. (d) The phosphorylation level of guard-cell PM H^+-ATPase estimated by immunohistochemical analyses. Isolated epidermal fragments were prepared from dark-treated plants and kept in the dark (Dk), illuminated with red light (600 μmol m^{-2} s^{-1}) for 30 min (RL), and illuminated with blue light (5 μmol m^{-2} s^{-1}) superimposed onto red light for 2.5 min after RL (RL→RB), or kept in the dark for 1 min after blue light illumination (RB→Dk) with 1.25 mM Na_2HPO_4, 2.5 mM $NaHCO_3$, or H_2O. Data represent the mean ± SD relative phosphorylation levels compared with Dk from four independent measurements. Asterisks indicate that the mean is significantly lower than that of RL→RB. *, $P < 0.05$; ns, $P > 0.1$ (one-tailed Dunnett's test). (e) Stomatal aperture analyses. The isolated epidermal fragments were kept in the dark, illuminated with blue light superimposed on red light for 2 h (RB), or kept in the dark for 10 min after RB (RB→Dk) with Na_2HPO_4, $NaHCO_3$ or H_2O. Chemical concentrations and light intensity were the same as in (d). Data represent the mean ± SD of three independent measurements. Asterisks indicate that the mean is significantly lower than that of RB. *, $P < 0.05$; ns, $P > 0.5$ (one-tailed Dunnett's test).

Next, we investigated stomatal movement in *ca1 ca4* by examining gas-exchange. Although the stomatal conductance in *ca1 ca4* was comparable with that of the wild-type at the beginning of the experiment, it was higher in *ca1 ca4* compared with the wild-type following red-light illumination (Fig. 4c,d), consistent with the higher phosphorylation level of guard-cell PM H^+-ATPase in the mutant leaves under red-light conditions (Fig. 4a, RL). Termination of the red-light illumination induced a decrease in stomatal conductance in both *ca1 ca4* and wild-type leaves; however, the rate of decrease was slower in *ca1 ca4* (Fig. 4c,e). Therefore, the stomatal conductance was higher in *ca1 ca4* than wild-type at 30 min after the light–dark transition (Fig. 4c,d). Photosynthesis was not impaired in *ca1 ca4* (Fig. 4c). A previous study showed that *ca1 ca4* exhibits increased stomatal density (Hu *et al.*, 2010); however, we did not observe the phenotype in this study (Fig. S7a). This might be due to the conditional effects during the plant growth. Therefore, the observed differences in stomatal responses were probably not caused by

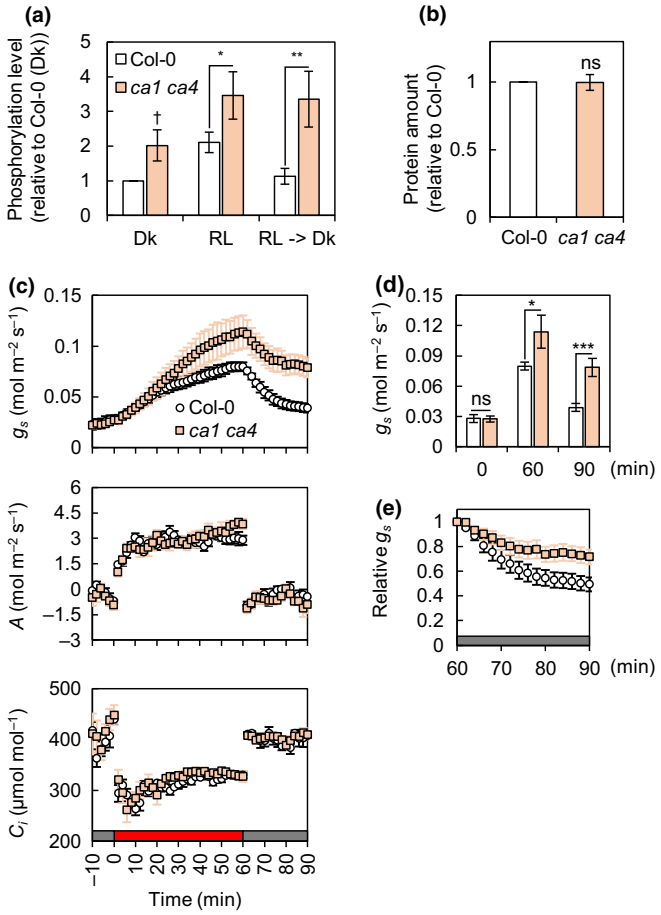

Fig. 4 Lack of both *CA1* and *CA4* delays dark-induced stomatal responses in *Arabidopsis thaliana* leaves. (a) Immunohistochemical analyses of the phosphorylation of plasma membrane (PM) H^+-ATPase in guard cells. Mature leaves harvested from dark-treated Col-0 and *ca1 ca4* plants were kept in the dark (Dk), illuminated with red light (600 μmol m^{-2} s^{-1}) for 30 min (RL), or kept in the dark for 1 min after RL (RL→Dk). Data represent mean ± SD relative phosphorylation levels compared with Col-0 (Dk) from three independent measurements. The dagger symbol denotes that the mean is significantly higher than Col-0 (Dk) set to 1. †, $P < 0.05$ (one-tailed one-sample *t*-test). Asterisks indicate that the mean of *ca1 ca4* is significantly higher than that of Col-0. *, $P < 0.05$; **, $P < 0.01$ (one-tailed Student's *t*-test). (b) Immunohistochemical analyses of the amount of PM H^+-ATPase in guard cells. Data represent the mean ± SD relative amounts of PM H^+-ATPase compared with Col-0 from three independent measurements. ns, mean is not significantly different from Col-0 set to 1. $P > 0.9$ (two-tailed one-sample *t*-test). (c–e) Gas-exchange analyses in Col-0 and *ca1 ca4*. Grey and red bars represent dark and red-light illumination conditions, respectively. The light intensity applied in this experiment was the same as in (a). (c) Stomatal conductance (g_s), photosynthetic rate (*A*) and intercellular CO_2 concentration (C_i). (d) g_s at each time point. Asterisks indicate that the mean of *ca1 ca4* is significantly higher than that of Col-0. *, $P < 0.05$; ***, $P < 0.001$; ns, $P > 0.5$ (one-tailed Student's *t*-test). (e) Relative g_s during the light–dark transition. g_s was normalised to the value at 60 min when the light was turned off. Data represent the mean ± SE of eight (Col-0) or seven (*ca1 ca4*) independent leaves from different plants.

differences in stomatal density. Taken together, these results indicated that *CA1* and *CA4* accelerated the dark-induced dephosphorylation of PM H^+-ATPase and stomatal closure.

HT1-mediated signal transduction is unlikely to function as a negative regulator for dark-induced dephosphorylation of guard-cell PM H^+-ATPase

The Raf-like protein kinase HT1 functions as a negative regulator of CO_2-induced stomatal closure downstream of CA1 and CA4 (Tian *et al.*, 2015; Hõrak *et al.*, 2016; Tõldsepp *et al.*, 2018). Thus, HT1 may function as a negative regulator of guard-cell PM H^+-ATPase dephosphorylation. Therefore, we expected the decrease in phosphorylation levels of guard-cell PM H^+-ATPase in the loss-of-function mutant. However, this phenotype was not present in a kinase-dead mutant *ht1-9* (Fig. S8a,b). Moreover, we did not detect any increases in phosphorylation levels of guard-cell PM H^+-ATPase in the dominant mutant *ht1-8D*, in which the CO_2-medited inhibition of HT1 is impaired (Hõrak *et al.*, 2016; Fig. S8a,b). In addition, a mutant plant lacking *CBC1* and *CBC2*, which also belong to the Raf-like kinases family and may be activated by HT1 to suppress CO_2-induced stomatal closure (Hiyama *et al.*, 2017), exhibited similar phenotypes to those of *ht1-9* (Fig. S8c,d). By contrast with *ht1-9* and *cbc1 cbc2* mutant plants, a mutant plant lacking *BHP*, another Raf-like kinase in guard cells (Hayashi *et al.*, 2017), exhibited decreased phosphorylation levels of guard-cell PM H^+-ATPase regardless of the light conditions (Fig. S9). Taken together, these results suggested that the HT1-mediated signal transduction does not function as a negative regulator of dark-induced guard-cell PM H^+-ATPase dephosphorylation.

OST1 does not affect the dark-induced dephosphorylation of PM H^+-ATPase in guard cells

ABA signalling affects CO_2-induced stomatal closure, even under nonstress conditions (Xue *et al.*, 2011; Merilo *et al.*, 2013; Chater *et al.*, 2015; Tian *et al.*, 2015; Hsu *et al.*, 2018; Dittrich *et al.*, 2019). *OST1* encodes a sucrose nonfermenting 1-related protein kinase (SnRK) 2, SnRK2.6, a core component of ABA signalling expressed in guard cells (Mustilli *et al.*, 2002; Yoshida *et al.*, 2002). In leaves of the knock-out mutant *ost1-3*, neither darkness nor elevated CO_2 levels induce rapid stomatal closure (Merilo *et al.*, 2013). Therefore, a lack of *OST1* might prevent the dephosphorylation of guard-cell PM H^+-ATPase and impair stomatal closure. However, there were no detectable dephosphorylation impairments in the guard-cell PM H^+-ATPase in *ost1-3* (Fig. S10a,b). Therefore, the dark-induced dephosphorylation of PM H^+-ATPase in guard cells may not require OST1 activity.

PP2C.D6 and D9 are required for dark-induced dephosphorylation of PM H^+-ATPase in guard cells

Recent studies have shown that PP2C.Ds dephosphorylate guard-cell PM H^+-ATPase to control stomatal aperture. Among nine isogenes of *PP2C.D*s, *PP2C.D6* and *PP2C.D9* are suggested to be major transcripts in guard cells (Wong *et al.*, 2021; Akiyama *et al.*, 2022). To evaluate the involvement of PP2C.D6 and/or D9 in the dark-induced dephosphorylation of guard-cell PM H^+-ATPase in leaves, we examined *pp2c.d6* and *d9* single

knock-out, and *pp2c.d6/9* double knock-out mutants. Interestingly, mutants lacking *PP2C.D6* (namely *pp2c.d6* and *d6/9*) failed to induce the rapid dephosphorylation of PM H^+-ATPase, whereas the *pp2c.d9* single knock-out mutants showed a response similar to the wild-type upon the light–dark transition (Fig. 5a). *pp2c.d6/9* leaves did not exhibit eCO_2-induced dephosphorylation of guard-cell PM H^+-ATPase (Fig. S6). There were no differences in the amount of PM H^+-ATPase between wild-type and mutant leaves (Fig. 5b). These results indicated that PP2C.D6 mediates the rapid dephosphorylation of guard-cell PM H^+-ATPase upon the light–dark transition. In addition, leaves maintained in the dark exhibited different properties. Dark-treated *pp2c.d6* and wild-type PM H^+-ATPase in guard cells exhibited comparable phosphorylation levels, whereas the phosphorylation levels in the dark-treated *pp2c.d9* and *pp2c.d6/9* leaves were almost twice as high as those of the wild-type; although, the increase in phosphorylation levels in *pp2c.d9* was not statistically significant (Fig. 5a, Dk). These results suggest that both PP2C.D6 and PP2C.D9 are required to maintain PM H^+-ATPase in a dephosphorylated state after the light–dark transition.

Next, we performed gas-exchange analyses to assess stomatal movement in *pp2c.d6* and *pp2c.d6/9*. At the beginning of the measurements, stomatal conductance was higher in *pp2c.d6/9* compared with the wild-type, while the stomatal conductance of *pp2c.d6* and wild-type were comparable (Fig. 5c,d). There were no significant differences in stomatal conductance between the wild-type and mutants under RL. In *pp2c.d6/9*, the dark-induced decrease in stomatal conductance was delayed, and the stomatal conductance was higher compared with the wild-type at 30 min after the light–dark transition (Fig. 5c–e). The decrease in stomatal conductance in *pp2c.d6* was similar to that of wild-type, although the stomatal conductance at 30 min after the light–dark transition was slightly higher in *pp2c.d6* compared with the wild-type (Fig. 5d,e). Each plant line showed similar photosynthetic rates and stomatal densities, which suggests that the observed differences in stomatal responses were not due to variations in photosynthetic capacity or stomatal density (Figs 5c, S7b). Taken together, these results indicated that *PP2C.D6* and *D9* control the rate of stomatal closure in leaves in the dark.

Discussion

By contrast with light-induced stomatal opening, knowledge regarding dark-induced stomatal closure is limited, and the early molecular mechanisms governing this process are yet to be elucidated. This study indicates that the dephosphorylation of guard-cell PM H^+-ATPase, accompanied by an increase in C_i, is an early molecular event in the course of dark-induced stomatal closure in leaves (Figs 1, 2). We genetically validated that constitutive activation of AHA1 results in impaired dark-induced stomatal closure in leaves, which suggests that deactivation of PM H^+-ATPase is probably required for stomatal closure upon the light–dark transition (Fig. S2). The phosphorylated penultimate residue of PM H^+-ATPase serves as a binding site for 14-3-3 protein, which is crucial for activation of PM H^+-ATPase in guard

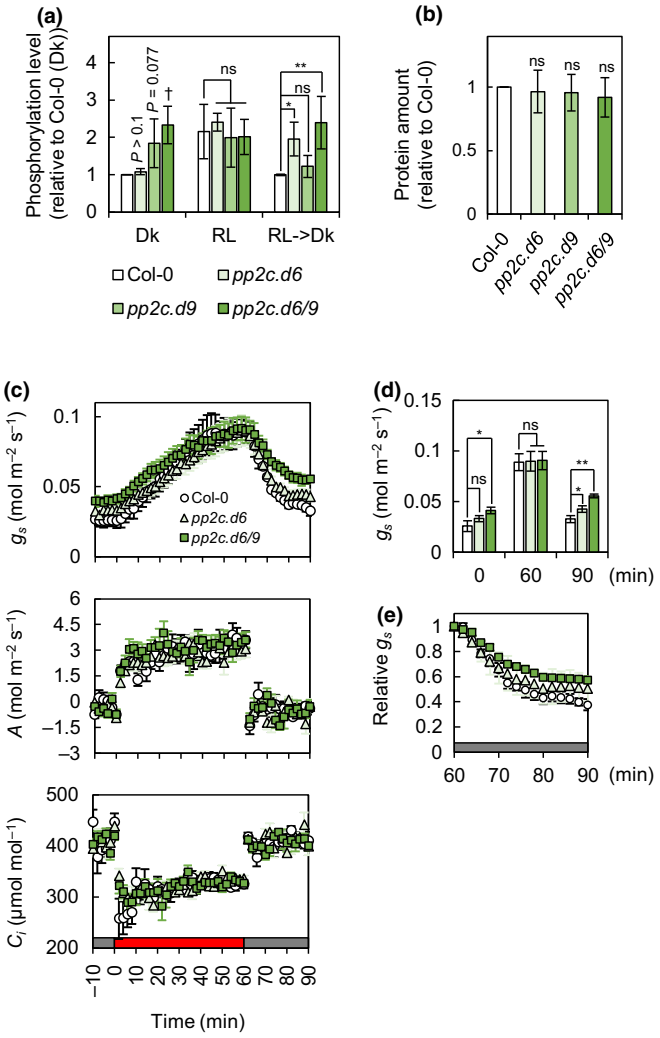

Fig. 5 PP2C.D6 and D9 regulate the dephosphorylation of guard-cell plasma membrane (PM) H^+-ATPase to promote stomatal closure in *Arabidopsis thaliana* leaves under the light–dark transition. (a) Immunohistochemical analyses of the phosphorylation of plasma membrane (PM) H^+-ATPase in guard cells. Mature leaves harvested from dark-treated Col-0, *pp2c.d6*, *d9* and *d6/9* plants were kept in the dark (Dk), illuminated with red light (600 μmol m^{-2} s^{-1}) for 30 min (RL), or kept in the dark for 1 min after RL (RL→Dk). Data represent mean ± SD relative phosphorylation levels compared with Col-0 (Dk) from three independent measurements. The dagger symbol denotes that the mean is significantly higher than Col-0 (Dk) set to 1. †, $P < 0.05$ (one-tailed one-sample *t*-test). Asterisks indicate that the mean value for the mutant is significantly higher than that of Col-0. *, $P < 0.05$; **, $P < 0.01$; ns, not significant, $P > 0.4$ (one-tailed Dunnett's test). (b) Immunohistochemical analyses of the amount of PM H^+-ATPase in guard cells. Data represent the mean ± SD relative amounts of PM H^+-ATPase compared with Col-0 from three independent measurements. ns, mean is not significantly different from Col-0 set to 1. $P > 0.9$ (two-tailed one-sample *t*-test). (c–e) Gas-exchange analyses in Col-0, *pp2c.d6* and *pp2c.d6/9*. Grey and red bars represent dark and red-light illumination conditions, respectively. The light intensity applied in this experiment was the same as in (a). (c) Stomatal conductance (g_s), photosynthetic rate (A) and intercellular CO_2 concentration (C_i). (d) g_s at each time point. Asterisks indicate that the mean value for the mutant is significantly higher than that of Col-0. *, $P < 0.05$; **, $P < 0.001$; ns, $P > 0.1$ (one-tailed Dunnett's test). (e) Relative g_s during the light–dark transition. g_s was normalised to the value at 60 min when the light was turned off. Data are the mean ± SE of four (Col-0), six (*pp2c.d6*), or five (*pp2c.d6/9*) independent leaves from different plants.

cells (Kinoshita & Shimazaki, 2002). Therefore, the delayed stomatal closure seen in mutant plants with dephosphorylation defects, such as *ca1 ca4* and *pp2c.d6/9* (Figs 4, 5), indicates that the rapid dephosphorylation of PM H^+-ATPase may facilitate deactivation of this enzyme and stomatal closure in the dark.

In this study, we found that elevated CO_2 levels induce the dephosphorylation of PM H^+-ATPase in guard cells (Figs 3, S4, S5). Impairment of dark- or eCO_2-induced dephosphorylation of guard-cell PM H^+-ATPase in *ca1 ca4* and *pp2c.d6/9* supports the hypothesis that CO_2 induces the dephosphorylation (Figs 4a, 5a, S6). Although previous evidence suggests that CO_2 inhibits PM H^+-ATPase in guard cells (Edwards & Bowling, 1985), the molecular mechanism behind this has not been investigated. This study suggests that CO_2 inhibits PM H^+-ATPase via dephosphorylation in guard cells.

A previous mathematical modelling suggested that the conversion of CO_2 into bicarbonate is delayed, not abolished, in guard cells lacking the CA activity; indeed, even *ca1 ca4* exhibited stomatal closure when the plants were exposed to prolonged eCO_2 conditions (Hu *et al.*, 2015). This may be the case in prolonged dark conditions as *ca1 ca4* and wild-type plants showed comparable stomatal conductance before light illumination, at which the plants had been kept in the dark overnight before the experiments (Fig. 4c). Moreover, increased phosphorylation level of guard-cell PM H^+-ATPase (Fig. 4a; Dk) may imply that some mechanisms counteract PM H^+-ATPase to achieve stomatal closure in the dark-treated *ca1 ca4*. Such a compensatory mechanism was found in mutant plants with a defect in the slow-type anion channel, in which elevated cytosolic Ca^{2+} and increased Ca^{2+} sensitivity of the inward-rectifying K^+ channel downregulate stomatal opening in the mutant guard cells (Laanemets *et al.*, 2013). Further investigations would be required to elucidate the compensatory mechanisms in *ca1 ca4*.

The molecular pathway that drives PM H^+-ATPase dephosphorylation, which is downstream of CA1 and CA4, may differ from the CO_2-mediated regulation of PM anion channels; our data suggest that the dephosphorylation is not regulated by HT1 and CBC inhibition (Fig. S8; Zhang *et al.*, 2018; Dubeaux *et al.*, 2021). Nevertheless, phosphorylation levels of guard-cell PM H^+-ATPase were somehow increased in the dark-treated *ht1-9* and *cbc1 cbc2* leaves (Fig. S8; Dk). Lack of these kinases' functions might have an indirect influence on PM H^+-ATPase phosphorylation, although mis-regulation of PM anion channels in the mutants is likely to antagonise PM H^+-ATPase to prevent stomatal opening (Hosotani *et al.*, 2021). Mesophyll cells also undergo photosynthesis-dependent PM H^+-ATPase phosphorylation under light; however, dark-induced dephosphorylation in mesophyll cells is slower than in guard cells, even though carbonic anhydrases are expressed in both types of cell (Hu *et al.*, 2010; Okumura *et al.*, 2016). This suggests that rapid dephosphorylation in guard cells may be mediated by guard-cell-rich components. HT1 and CBCs belong to the family of Raf-like kinases (Hayashi *et al.*, 2020). Another Raf-like kinase expressed in guard cells, BHP regulates the blue light-induced phosphorylation of guard-cell PM H^+-ATPase in isolated epidermal fragments and GCPs (Hayashi *et al.*, 2017). Interestingly, we found that the phosphorylation level of guard-cell PM H^+-ATPase in the leaves of a *bhp-1* knock-out mutant was lower than that of the wild-type, regardless of the light conditions (Fig. S9). This suggests that BHP could be a negative regulator of rapid guard-cell PM H^+-ATPase dephosphorylation, which should be investigated in future studies.

Recent biochemical and live-imaging analyses indicated that CO_2 does not trigger an increase in ABA levels or activate OST1 in guard cells; therefore, CO_2-induced stomatal closure may be independent of ABA signalling and stimulated downstream of OST1 (Hsu *et al.*, 2018; Zhang *et al.*, 2020). Given that dark-induced guard-cell PM H^+-ATPase dephosphorylation occurs in response to CO_2 levels, the occurrence of dark-induced guard-cell PM H^+-ATPase dephosphorylation in *ost1-3* suggests that it may not be a downstream target of OST1 during dark-induced stomatal closure (Fig. S10). A recent study suggested that ABA is not essential in dark-induced stomatal closure (Pridgeon & Hetherington, 2021). Presence of dark-induced dephosphorylation of PM H^+-ATPase in *ost1-3* implies that ABA might not be essential in the dephosphorylation. Future studies could be expanded to other ABA signalling components to elucidate this.

Rapid PM H^+-ATPase dephosphorylation did not occur in the guard cells of mutants *pp2c.d6* or *pp2c.d6/9* following the light–dark transition; however, guard-cell PM H^+-ATPase of *pp2c.d6* was dephosphorylated when maintained in dark conditions (Fig. 5a). Similarly, *pp2c.d6/9* exhibited delayed stomatal closure in the dark, while stomatal closure was barely affected in *pp2c.d6* (Fig. 5c–e). Taken together, our results suggested that PP2C.D6 initiates dephosphorylation upon light–dark transition and PP2C.D9 then maintains the PM H^+-ATPase in a dephosphorylated state to promote rapid stomatal closure. A recent study indicated that PP2C.D2 and D5, as well as D6, regulate stomatal movement (Wong *et al.*, 2021). The role of PP2C.D isoforms in dark-induced PM H^+-ATPase dephosphorylation in guard cells should be explored in future studies. In addition, how PP2C.Ds are regulated by dark conditions and/or CO_2 is currently unknown. PP2C.Ds are inhibited by SMALL AUXIN UP RNAs (SAURs), which in turn regulate PM H^+-ATPase phosphorylation in seedlings (Spartz *et al.*, 2014). Notably, stomatal opening is suppressed in *saur56 saur60* (Wong *et al.*, 2021). The involvement of SAURs in rapid dark-induced PM H^+-ATPase dephosphorylation in guard cells should be investigated in future studies.

Based on the results of this study, we propose a new model of stomatal closure in leaves involving CO_2-induced rapid PM H^+-ATPase dephosphorylation, which occurs alongside CO_2-mediated activation of PM anion channels in guard cells (Fig. 6). Although the genetic relationship between carbonic anhydrases and PP2C.D6/9 should be confirmed in future work, our findings highlighted how guard-cell PM H^+-ATPase, a driver of stomatal opening, is regulated in response to the dark or CO_2, leading to stomatal closure in leaves. This study also reports a novel mechanism of plant responses to CO_2. eCO_2 and $NaHCO_3$ treatments induced dephosphorylation even in the light (Figs 3b, S4). Interestingly, $NaHCO_3$-induced dephosphorylation under blue light was slightly delayed compared with

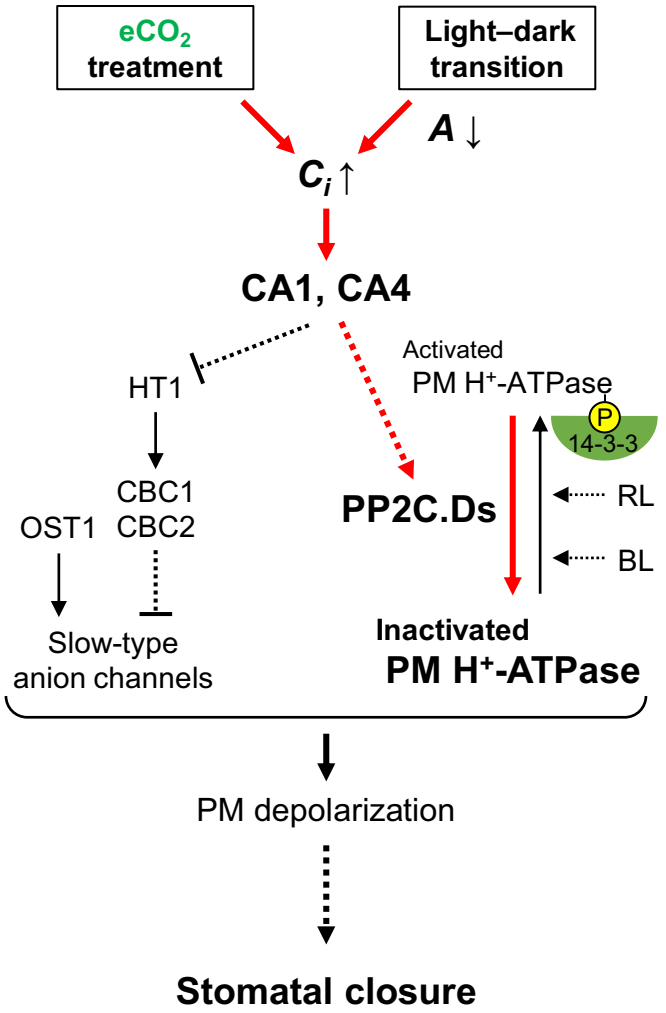

Fig. 6 Putative model of the early processes of stomatal closure in leaves, involving CO_2-mediated regulation of plasma membrane (PM) H^+-ATPase in guard cells. The increase in intercellular CO_2 concentration (C_i ↑), which is caused by the cessation of photosynthesis (A ↓) under the light–dark transition or elevated CO_2 treatment, induces the dephosphorylation of PM H^+-ATPase, which would prevent 14-3-3 binding and lead to inactivation of PM H^+-ATPase (Kinoshita & Shimazaki, 2002). The dephosphorylation probably requires the activity of carbonic anhydrases CA1 and CA4, and may be catalysed at least by PP2C.D6 and PP2C.D9. Blue light (BL)- and red light (RL)-induced phosphorylation of PM H^+-ATPase (Kinoshita & Shimazaki, 1999; Ando & Kinoshita, 2018), which are likely to be independent of C_i, may compete against the dephosphorylation. Along with carbonic anhydrase-mediated activation of PM anion channels, inactivation of PM H^+-ATPase by dephosphorylation may efficiently induce PM depolarization in guard cells, prompting the release of solutes from the cells and subsequent stomatal closure (Roelfsema *et al*., 2012; Zhang *et al*., 2018; Dubeaux *et al*., 2021). Red lines show the signal transduction pathways suggested in this study. Dotted lines indicate omitted or unidentified signalling components. Arrows and T-bars represent positive and negative regulation, respectively.

that in the dark (Fig. S4). This delay may be explained by competition between blue light-induced phosphorylation and CO_2-meidated dephosphorylation of PM H^+-ATPase in guard cells. eCO_2-induced dephosphorylation under RL was also slightly delayed and required higher level of C_i compared with the dephosphorylation upon the light–dark transition (Fig. 3b). This may imply that red-light-induced phosphorylation of guard-cell PM H^+-ATPase is a C_i-independent response and competes with the dephosphorylation. This hypothesis would be consistent with the idea that red-light-induced stomatal opening is mediated both by C_i-dependent and C_i-independent mechanisms (Matrosova *et al*., 2015). Therefore, we consider that the phosphorylation level of guard-cell PM H^+-ATPase may be regulated both by C_i-dependent dephosphorylation and C_i-independent light-induced phosphorylation (Fig. 6). Furthermore, the model suggests that fluctuations in photosynthetic activity during the daytime, which occurs due to the fluctuating light conditions (Tanaka *et al*., 2019), may be a matter for the regulation of stomatal movement in the field. Rapid stomatal closure might prevent deterioration in plant water use efficiency when the photosynthetic capacity is lowered. Future investigations could explore how stomatal movement is regulated in unstable light environments.

Acknowledgements

Seeds of *ca1 ca4* were kindly provided by Dr Julian I. Schroeder (University of California, San Diego). Seeds of *cbc1 cbc2* and *ht1-9* were kindly provided by Dr Ken-ichiro Shimazaki (Kyushu University). We thank Dr Masaru Kono (The University of Tokyo) for technical advice. We also thank Ms Kyomi Taki (Nagoya University) for technical assistance. This work was supported by a Grant-in-Aid for Japan Society for the Promotion of Science Research Fellow (grant no. 20 J00392 to EA) and Grants-in-Aid for Scientific Research from the Ministry of Education, Culture, Sports, Science and Technology, Japan (grant nos. 20H05687 and 20H05910 to TK).

Author contributions

EA, HK and TK designed the research; EA, KF and TK performed the research; and EA, HK, KF, TK and IT wrote the article.

ORCID

Eigo Ando https://orcid.org/0000-0001-6232-6573
Toshinori Kinoshita https://orcid.org/0000-0001-7621-1259
Hannes Kollist https://orcid.org/0000-0002-6895-3583
Ichiro Terashima https://orcid.org/0000-0001-7680-9867

Data availability

The data that support the findings of this study are available from TK upon reasonable request.

References

Akiyama M, Sugimoto H, Inoue S, Takahashi Y, Hayashi M, Hayashi Y, Mizutani M, Ogawa T, Kinoshita D, Ando E *et al.* 2022. Type 2C protein phosphatase clade D family members dephosphorylate guard cell plasma membrane H^+-ATPase. *Plant Physiology* **188**: 2228–2240.

Ando E, Kinoshita T. 2018. Red light-induced phosphorylation of plasma membrane H^+-ATPase in stomatal guard cells. *Plant Physiology* **178**: 836–849.

Brearley J, Venis MA, Blatt MR. 1997. The effect of elevated CO_2 concentration on K^+ and anion channels of *Vicia faba* L. guard cells. *Planta* **203**: 145–154.

Chater C, Peng K, Movahedi M, Dunn JA, Walker HJ, Liang YK, McLachlan DH, Casson S, Isner JC, Wilson I *et al.* 2015. Elevated CO_2-induced responses in stomata require ABA and ABA signaling. *Current Biology* **25**: 2709–2716.

Chikov VI, Akhtyamova GA. 2019. Photorespiration and its role in the regulation of photosynthesis and plant productivity. *American Journal of Plant Sciences* **10**: 2179–2202.

Daloso DM, Dos Anjos L, Fernie AR. 2016. Roles of sucrose in guard cell regulation. *New Phytologist* **211**: 809–818.

Desikan R, Cheung MK, Clarke A, Golding S, Sagi M, Fluhr R, Rock C, Hancock J, Neill S. 2004. Hydrogen peroxide is a common signal for darkness- and ABA-induced stomatal closure in *Pisum sativum*. *Functional Plant Biology* **31**: 913–920.

Dittrich M, Mueller HM, Bauer H, Peirats-Llobet M, Rodriguez PL, Geilfus CM, Carbentier SC, Al Rasheid KAS, Kollist H, Merilo E *et al.* 2019. The role of Arabidopsis ABA receptors from the PYR/PYL/RCAR family in stomatal acclimation and closure signal integration. *Nature Plants* **5**: 1002–1011.

Dubeaux G, Hsu PK, Ceciliato PHO, Swink KJ, Rappel WJ, Schroeder JI. 2021. Deep dive into CO_2-dependent molecular mechanisms driving stomatal responses in plants. *Plant Physiology* **187**: 2032–2042.

Edwards A, Bowling DJF. 1985. Evidence for a CO_2 inhibited proton extrusion pump in the stomatal cells of *Tradescantia virginiana*. *Journal of Experimental Botany* **36**: 91–98.

Eisinger W, Ehrhardt D, Briggs W. 2012. Microtubules are essential for guard-cell function in *Vicia* and *Arabidopsis*. *Molecular Plant* **5**: 601–610.

Engineer CB, Hashimoto-Sugimoto M, Negi J, Israelsson-Nordström M, Azoulay-Shemer T, Rappel WJ, Iba K, Schroeder JI. 2016. CO_2 sensing and CO_2 regulation of stomatal conductance: advances and open questions. *Trends in Plant Science* **21**: 16–30.

Flütsch S, Wang Y, Takemiya A, Vialet-Chabrand SRM, Klejchová M, Nigro A, Hills A, Lawson T, Blatt MR, Santelia D. 2020. Guard cell starch degradation yields glucose for rapid stomatal opening in Arabidopsis. *Plant Cell* **32**: 2325–2344.

Fujita T, Noguchi K, Ozaki H, Terashima I. 2019. Confirmation of mesophyll signals controlling stomatal responses by a newly devised transplanting method. *Functional Plant Biology* **46**: 467–481.

Fujita T, Noguchi K, Terashima I. 2013. Apoplastic mesophyll signals induce rapid stomatal responses to CO_2 in *Commelina communis*. *New Phytologist* **199**: 395–406.

Goh CH, Ko SM, Park YI, Kim CS, Song KJ. 2011. Regulation of dark-induced stomatal closure in *Arabidopsis* dynamin-like protein 1E (*adl1e*) mutant leaves. *Journal of Plant Biology* **54**: 112–118.

Granot D, Kelly G. 2019. Evolution of guard-cell theories: the story of sugars. *Trends in Plant Science* **24**: 507–518.

Hashimoto M, Negi J, Young J, Israelsson M, Schroeder JI, Iba K. 2006. *Arabidopsis* HT1 kinase controls stomatal movements in response to CO_2. *Nature Cell Biology* **8**: 391–397.

Hayashi M, Inoue S, Takahashi K, Kinoshita T. 2011. Immunohistochemical detection of blue light-induced phosphorylation of the plasma membrane H^+-ATPase in stomatal guard cells. *Plant and Cell Physiology* **52**: 1238–1248.

Hayashi M, Inoue S, Ueno Y, Kinoshita T. 2017. A raf-like protein kinase BHP mediates blue light-dependent stomatal opening. *Scientific Reports* **7**: 45586.

Hayashi M, Sugimoto H, Takahashi H, Seki M, Shinozaki K, Sawasaki T, Kinoshita T, Inoue S. 2020. Raf-like kinases CBC1 and CBC2 negatively regulate stomatal opening by negatively regulating plasma membrane H^+-ATPase phosphorylation in *Arabidopsis*. *Photochemical and Photobiological Sciences* **19**: 88–98.

Hayashi Y, Nakamura S, Takemiya A, Takahashi Y, Shimazaki K, Kinoshita T. 2010. Biochemical characterization of *in vitro* phosphorylation and dephosphorylation of the plasma membrane H^+-ATPase. *Plant and Cell Physiology* **51**: 1186–1196.

Hiyama A, Takemiya A, Munemasa S, Okuma E, Sugiyama N, Tada Y, Murata Y, Shimazaki K. 2017. Blue light and CO_2 signals converge to regulate light-induced stomatal opening. *Nature Communications* **8**: 1284.

Hõrak H, Sierla M, Tõldsepp K, Wang C, Wang YS, Nuhkat M, Valk E, Pechter P, Merilo E, Salojärvi J *et al.* 2016. A dominant mutation in the HT1 kinase uncovers roles of MAP kinases and GHR1 in CO_2-indced stomatal closure. *Plant Cell* **28**: 2493–2509.

Horrer D, Flütsch S, Pazmino D, Matthews JSA, Thalmann M, Nigro A, Leonhardt N, Lawson T, Santelia D. 2016. Blue light induces a distinct starch degradation pathway in guard cells for stomatal opening. *Current Biology* **26**: 362–370.

Hosotani S, Yamauchi S, Kobayashi H, Fuji S, Koya S, Shimazaki K, Takemiya A. 2021. A BLUS1 kinase signal and a decrease in intercellular CO_2 concentration are necessary for stomatal opening in response to blue light. *Plant Cell* **33**: 1813–1827.

Hothorn T, Bretz F, Westfall P. 2008. Simultaneous inference in general parametric models. *Biometrical Journal* **50**: 346–363.

Hsu PK, Takahashi Y, Munemasa S, Merilo E, Laanemets K, Waadt R, Pater D, Kollist H, Schroeder JI. 2018. Abscisic acid-independent stomatal CO_2 signal transduction pathway and convergence of CO_2 and ABA signaling downstream of OST1 kinase. *Proceedings of the National Academy of Sciences, USA* **115**: E9971–E9980.

Hu H, Boisson-Dernier A, Israelsson-Nordström M, Böhmer M, Xue S, Ries A, Godoski J, Kuhn JM, Schroeder JI. 2010. Carbonic anhydrases are upstream regulators of CO_2-controlled stomatal movements in guard cells. *Nature Cell Biology* **12**: 87–93.

Hu H, Rappel WJ, Occhipinti R, Ries A, Böhmer M, You L, Xiao C, Engineer CB, Boron WF, Schroeder JI. 2015. Distinct cellular locations of carbonic anhydrases mediate carbon dioxide control of stomatal movements. *Plant Physiology* **169**: 1168–1178.

Inoue S, Kinoshita T. 2017. Blue light regulation of stomatal opening and the plasma membrane H^+-ATPase. *Plant Physiology* **174**: 531–538.

Isner JC, Xu Z, Costa JM, Monnet F, Batstone T, Ou X, Deeks MJ, Genty B, Jiang K, Hetherington AM. 2017. Actin filament reorganization controlled by the SCAR/WAVE complex mediates stomatal response to darkness. *New Phytologist* **215**: 1059–1067.

Jalakas P, Nuhkat M, Vahisalu T, Merilo E, Brosché M, Kollist H. 2021. Combined action of guard cell plasma membrane rapid- and slow-type anion channels in stomatal regulation. *Plant Physiology* **187**: 2126–2133.

Jezek M, Blatt MR. 2017. The membrane transport system of the guard cell and its integration for stomatal dynamics. *Plant Physiology* **174**: 487–519.

Kang CY, Lian HL, Wang FF, Huang JR, Yang HQ. 2009. Cryptochromes, phytochromes, and COP1 regulate light-controlled stomatal development in Arabidopsis. *Plant Cell* **21**: 2624–2641.

Khanna R, Li J, Tseng TS, Schroeder JI, Ehrhardt DW, Briggs WR. 2014. COP1 jointly modulates cytoskeletal processes and electrophysiological responses required for stomatal closure. *Molecular Plant* **7**: 1441–1454.

Kinoshita T, Doi M, Suetsugu N, Kagawa T, Wada M, Shimazaki K. 2001. phot1 and phot2 mediate blue light regulation of stomatal opening. *Nature* **414**: 656–660.

Kinoshita T, Shimazaki K. 1999. Blue light activates the plasma membrane H^+-ATPase by phosphorylation of the C-terminus in stomatal guard cells. *EMBO Journal* **18**: 5548–5558.

Kinoshita T, Shimazaki K. 2002. Biochemical evidence for the requirement of 14-3-3 protein binding in activation of the guard-cell plasma membrane H^+-ATPase by blue light. *Plant and Cell Physiology* **43**: 1359–1365.

Kolla VA, Vavasseur A, Raghavendra AS. 2007. Hydrogen peroxide production is an early event during bicarbonate induced stomatal closure in abaxial epidermis of *Arabidopsis*. *Planta* **225**: 1421–1429.

Laanemets K, Wang YF, Lindgren O, Wu J, Nishimura N, Lee S, Caddell D, Merilo E, Brosche M, Kilk K *et al.* 2013. Mutations in the SLAC1 anion channel slow stomatal opening and severely reduce K^+ uptake channel activity via enhanced cytosolic $[Ca^{2+}]$ and increased Ca^{2+} sensitivity of K^+ uptake channels. *New Phytologist* **197**: 88–98.

Lawson T, Lefebvre S, Baker NR, Morison JIL, Raines CA. 2008. Reductions in mesophyll and guard cell photosynthesis impact on the control of stomatal responses to light and CO_2. *Journal of Experimental Botany* **59**: 3609–3619.

Lawson T, Matthews J. 2020. Guard cell metabolism and stomatal function. *Annual Review of Plant Biology* **71**: 273–302.

Liang YK, Dubos C, Dodd IC, Holroyd GH, Hetherington AM, Campbell MM. 2005. *At*MYB61, an R2R3-MYB transcription factor controlling stomatal aperture in *Arabidopsis thaliana*. *Current Biology* **15**: 1201–1206.

Ma YL, She XP, Yang SS. 2012. Sphingosine-1-phosphate (S1P) mediates darkness-induced stomatal closure through raising cytosol pH and hydrogen peroxide (H_2O_2) levels in guard cells in *Vicia faba*. *Science China Life Sciences* **55**: 974–983.

Mao J, Zhang YC, Sang Y, Li QH, Yang HQ. 2005. A role for *Arabidopsis* cryptochromes and COP1 in the regulation of stomatal opening. *Proceedings of the National Academy of Sciences, USA* **102**: 12270–12275.

Marten H, Hedrich R, Roelfsema MRG. 2007. Blue light inhibits guard cell plasma membrane anion channels in a phototropin-dependent manner. *The Plant Journal* **50**: 29–39.

Matrosova A, Bogireddi H, Mateo-Peñas A, Hashimoto-Sugimoto M, Iba K, Schroeder JI, Israelsson-Nordström M. 2015. The HT1 protein kinase is essential for red light-induced stomatal opening and genetically interacts with OST1 in red light and CO_2-induced stomatal movement responses. *New Phytologist* **208**: 1126–1137.

McLachlan DH, Lan J, Geilfus CM, Dodd AN, Larson T, Baker A, Hõrak H, Kollist H, He Z, Graham I *et al.* 2016. The breakdown of stored triacylglycerols is required during light-induced stomatal opening. *Current Biology* **26**: 707–712.

Merilo E, Laanemets K, Hu H, Xue S, Jakobson L, Tulva I, Gonzalez-Guzman M, Rodriguez PL, Shroeder JI, Broschè M *et al.* 2013. PYR/RCAR receptors contribute to ozone-, reduced air humidity- darkness- and CO_2-induced stomatal regulation. *Plant Physiology* **162**: 1652–1668.

Merlot S, Leonhardt N, Fenzi F, Valon C, Costa M, Piette L, Vavasseur A, Genty B, Boivin K, Müller A *et al.* 2007. Constitutive activation of a plasma membrane H^+-ATPase prevents abscisic acid-mediated stomatal closure. *EMBO Journal* **26**: 3216–3226.

Messinger SM, Buckley TN, Mott KA. 2006. Evidence for involvement of photosynthetic processes in the stomatal response to CO_2. *Plant Physiology* **140**: 771–778.

Mott KA, Sibbernsen ED, Shope JC. 2008. The role of the mesophyll in stomatal responses to light and CO_2. *Plant, Cell & Environment* **31**: 1299–1306.

Mustilli AC, Merlot S, Vavasseur A, Fenzi F, Giraudat J. 2002. Arabidopsis OST1 protein kinase mediates the regulation of stomatal aperture by abscisic acid and acts upstream of reactive oxygen species production. *Plant Cell* **14**: 3089–3099.

Negi J, Matsuda O, Nagasawa T, Oba Y, Takahashi H, Kawai-Yamada M, Uchimiya H, Hashimoto M, Iba K. 2008. CO_2 regulator SLAC1 and its homologues are essential for anion homeostasis in plant cells. *Nature* **452**: 483–486.

Okumura M, Inoue S, Kuwata K, Kinoshita T. 2016. Photosynthesis activates plasma membrane H^+-ATPase via sugar accumulation. *Plant Physiology* **171**: 580–589.

Pridgeon AJ, Hetherington AM. 2021. ABA signalling and metabolism are not essential for dark-induced stomatal closure but affect response speed. *Scientific Reports* **11**: 5751.

R Core Team. 2021. *R: a language and environment for statistical computing*. Vienna, Austria: R Foundation for Statistical Computing.

Roelfsema MRG, Hanstein S, Felle HH, Hedrich R. 2002. CO_2 provides an intermediate link in the red light response of guard cells. *The Plant Journal* **32**: 65–75.

Roelfsema MRG, Hedrich R, Geiger D. 2012. Anion channels: master switches of stress responses. *Trends in Plant Science* **17**: 221–229.

Santelia D, Lunn JE. 2017. Transitory starch metabolism in guard cell: unique features for a unique function. *Plant Physiology* **174**: 539–549.

Schneider CA, Rasband WS, Eliceiri KW. 2012. NIH Image to ImageJ: 25 years of image analysis. *Nature Methods* **9**: 671–675.

She XP, Huang AX, Li J, Han XZ. 2010. Inhibition of dark-induced stomatal closure by fusicoccin involves a removal of hydrogen peroxide in guard cells of *Vicia faba*. *Physiologia Plantarum* **140**: 258–268.

Shimazaki K, Doi M, Assmann SM, Kinoshita T. 2007. Light regulation of stomatal movement. *Annual Review of Plant Biology* **58**: 219–247.

Spartz AK, Ren H, Park MY, Grandt KN, Lee SH, Murphy AS, Sussman MR, Overvoorde PJ, Gray WM. 2014. SAUR inhibition of PP2C-D phosphatases activates plasma membrane H^+-ATPases to promote cell expansion in *Arabidopsis*. *Plant Cell* **26**: 2129–2142.

Suetsugu N, Takami T, Ebisu Y, Watanabe H, Iiboshi C, Doi M, Shimazaki K. 2014. Guard cell chloroplasts are essential for blue light-dependent stomatal opening in Arabidopsis. *PLoS ONE* **9**: e108374.

Tanaka Y, Adachi S, Yamori W. 2019. Natural genetic variation of the photosynthetic induction response to fluctuating light environment. *Current Opinion in Plant Biology* **49**: 52–59.

Tian W, Hou C, Ren Z, Pan Y, Jia J, Zhang H, Bai F, Zhang P, Zhu H, He Y *et al.* 2015. A molecular pathway for CO_2 response in *Arabidopsis* guard cells. *Nature Communications* **6**: 6057.

Tõldsepp K, Zhang J, Takahashi Y, Sindarovska Y, Hõrak H, Ceciliato PHO, Koolmeister K, Wang YS, Vaahtera L, Jakobson L *et al.* 2018. Mitogen-activated protein kinases MPK4 and MPK12 are key components mediating CO_2-induced stomatal movements. *The Plant Journal* **96**: 1018–1935.

Tominaga M, Kinoshita T, Shimazaki K. 2001. Guard-cell chloroplasts provide ATP required for H^+ pumping in the plasma membrane and stomatal opening. *Plant and Cell Physiology* **42**: 795–802.

Ueno K, Kinoshita T, Inoue S, Emi T, Shimazaki K. 2005. Biochemical characterization of plasma membrane H^+-ATPase activation in guard cell protoplasts of *Arabidopsis thaliana* in response to blue light. *Plant and Cell Physiology* **46**: 955–963.

Vahisalu T, Kollist H, Wang YF, Nishimura N, Chan WY, Valerio G, Lamminmäki A, Brosché M, Moldau H, Desikan R *et al.* 2008. SLAC1 is required for plant guard cell S-type anion channel function in stomatal signalling. *Nature* **452**: 487–491.

Wang SW, Li Y, Zhang XL, Yang HQ, Han XF, Liu ZH, Shang ZL, Asano T, Yoshioka Y, Zhang CG *et al.* 2014. Lacking chloroplasts in guard cells of crumpled leaf attenuates stomatal opening: both guard cell chloroplasts and mesophyll contribute to guard cell ATP levels. *Plant, Cell & Environment* **37**: 2201–2210.

Wong JH, Klejchová M, Snipes SA, Nagpal P, Bak G, Wang B, Dunlap S, Park MY, Kunkel EN, Trinidad B *et al.* 2021. SAUR proteins and PP2C.D phosphatases regulate H^+-ATPases and K^+ channels to control stomatal movements. *Plant Physiology* **185**: 256–273.

Xue S, Hu H, Ries A, Merilo E, Kollist H, Schroeder JI. 2011. Central functions of bicarbonate in S-type anion channel activation and OST1 protein kinase in CO_2 signal transduction in guard cell. *EMBO Journal* **30**: 1645–1658.

Yamauchi S, Takemiya A, Sakamoto T, Kurata T, Tsutsumi T, Kinoshita T, Shimazaki K. 2016. The plasma membrane H^+-ATPase AHA1 plays a major role in stomatal opening in response to blue light. *Plant Physiology* **171**: 2731–2743.

Yoshida R, Hobo T, Ichimura K, Mizoguchi T, Takahashi F, Aronso J, Ecker JR, Shinozaki K. 2002. ABA-activated SnRK2 protein kinase is required for dehydration stress signaling in *Arabidopsis*. *Plant and Cell Physiology* **43**: 1473–1483.

Zhang J, De-oliveira-Ceciliato P, Takahashi Y, Schulze S, Dubeaux G, Hauser F, Azoulay-Shemer T, Tõldsepp K, Kollist H, Rappel WJ *et al.* 2018. Insights into the molecular mechanisms of CO_2-mediated regulation of stomatal movements. *Current Biology* **28**: R1356–R1363.

Zhang L, Takahashi Y, Hsu PK, Kollist H, Merilo E, Krysan PJ, Schroeder JI. 2020. FRET kinase sensor development reveals SnRK2/OST1 activation by ABA but not by MeJA and high CO_2 during stomatal closure. *eLife* **9**: e56351.

Supporting Information

Additional Supporting Information may be found online in the Supporting Information section at the end of the article.

Fig. S1 Guard cells in isolated epidermal fragments lack rapid responses to dark conditions.

Fig. S2 Dark-induced stomatal closure is abolished in *Arabidopsis thaliana ost2-1* leaves.

Fig. S3 Ambient CO_2 concentration (C_a), photosynthetic rate (A), intercellular CO_2 concentration (C_i) and stomatal conductance (g_s) in *Arabidopsis thaliana* wild-type Col-0 leaves recorded in the experiment shown in Fig. 3(a–c).

Fig. S4 Blue light slightly delays $NaHCO_3$-induced dephosphorylation of guard-cell plasma membrane H^+-ATPase in *Arabidopsis thaliana* wild-type Col-0 epidermal fragments.

Fig. S5 $NaHCO_3$-induced dephosphorylation of plasma membrane H^+-ATPase in *Arabidopsis thaliana* wild-type Col-0 guard-cell protoplasts.

Fig. S6 Elevated CO_2 (eCO_2)-induced dephosphorylation of guard-cell plasma membrane H^+-ATPase is impaired in *Arabidopsis thaliana ca1 ca4* and *pp2c.d6/9* leaves.

Fig. S7 Stomatal density of *Arabidopsis thaliana* leaves used for the gas-exchange analyses.

Fig. S8 *HT1*, *CBC1* and *CBC2* are not likely to function as a negative regulator of dark-induced dephosphorylation of guard-cell plasma membrane H^+-ATPase in *Arabidopsis thaliana* leaves.

Fig. S9 The phosphorylation of guard-cell plasma membrane H^+-ATPase is suppressed in *Arabidopsis thaliana bhp-1* leaves under all light conditions tested.

Fig. S10 Dark-induced dephosphorylation of guard-cell plasma membrane H^+-ATPase is not impaired in *Arabidopsis thaliana ost1-3* leaves.

Please note: Wiley Blackwell are not responsible for the content or functionality of any Supporting Information supplied by the authors. Any queries (other than missing material) should be directed to the *New Phytologist* Central Office.